

The Komberek karst area - An example of the basement rock influence on the morphology of karst sinkholes (Malé Karpaty Mts., Slovakia)

Alexander Lačný^{1,2}, Michal Šujan¹, Jozef Hók¹, Tamás Csibri¹, René Putiška³, Ivan Dostál³, Andrej Mojzeš³

¹ Comenius University, Faculty of Natural Sciences, Department of Geology and Paleontology, Ilkovičova 6, Bratislava, Slovakia, e-mail: alexander.lacny@uniba.sk

² State Nature Conservancy of the Slovak Republic, Little Carpathians Protected Landscape Area, Štúrova 115, 900 01, Modra, Slovakia

³ Comenius University, Faculty of Natural Sciences, Department of Applied and Environmental Geophysics, Ilkovičova 6, Bratislava, Slovakia

AGEOS

Abstract: The studied area, as the part of the Malé Karpaty Mts., is an integral part of the Western Carpathian orogenic belt. The Komberek karst area is built up by the Tatricum and Fatricum tectonic units. The studied area belongs to the Kuchyňa-Orešany Karst, where on the northeastern part the karst plain Komberek (Křč) Hill (409 m a.s.l.) is situated. During the research, geological (geological mapping), geophysical (electrical resistivity tomography-ERT and soil radon emanometry) and sedimentological (shallow drilling) methods were carried out. This combination of methods allows to interpret the origin and morphology of the sinkholes. The morphology depends on the nature of the basement rocks, the sedimentary cover and the tectonic influence. Funnel-shaped and pot-like sinkholes are concentrated into a sinkhole line located in a linear NW–SE-trending structure line. In the other side, some sinkholes were formed on the lithological boundary of the karstic and nonkarstic rocks. Moreover, the sinkholes are at the edge of the depression filled with fine-grained impermeable sediments. In addition, this study points out to the possible presence of potential cavity spaces under one of the largest sinkholes found on the karst plateau.

Key words: sinkholes, linear discontinuity, ERT method, soil radon emanometry

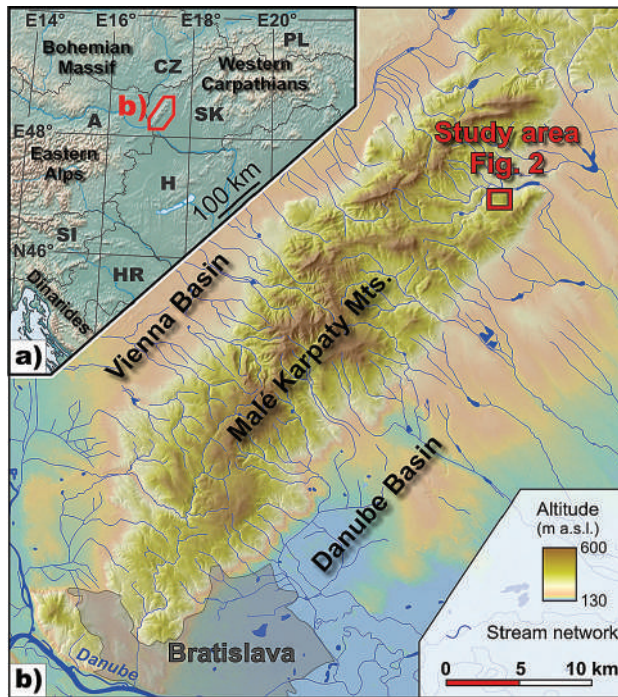
1. INTRODUCTION

The sinkholes are the most specific surface forms of the karst relief. They form closed depressions of variable dimensions with slightly inclined to almost vertical side walls (Bondesan et al., 1992; Williams, 2004). From a morphodynamic point of view, they form a basic hydrographic unit that acts as a simple catchment, that drives water to its lowest accumulation point by using its slope system. The genesis of the karst sinkholes is influenced by topographic and morphostructural predisposition. For this reason, they can arise through multiple processes. In general, four main mechanisms of karst sinkhole formation are recognized (corrosion, collapse, suffosion and subsidence), but the formation of karst sinkholes cannot always be connected to one of these processes. That is why they are described as polygenetic forms of the relief. Depending on the process, various shapes of karst sinkholes may occur, they are either isolated or appear in groups. Since international terminology uses multiple concepts to designate genetic types of karst sinkholes. Williams (2004) for example assigns individual terms to a particular genetic process. Jakál (1975) on the other hand used the classification with 2 genetic types of sinkholes: a.) sinkholes resulted from collapse of karst structures, and b.) sinkholes created by water corrosion. He also divides the sinkholes according to their slope dips into four categories (funnel-shaped, spherical, pot-like and annular). Morphometric analysis is a quantification tool for generating hypotheses about the evolution and dynamics of karst geosystem

and surrounding landscape. The genesis of the sinkholes also depends on the basement type and on tectonic processes that influenced them. Adequate analysis of sinkhole genesis requires combination of numerous methods, including morphometrical analysis, basement rock analysis, as well as analysis of subsurface conditions, provided by geophysical methods. The present study offers such approach and deals with the different factors of sinkhole genesis and with complicated geological conditions in the Komberek karst plateau. The following results and their implications will provide and comprehensive workflow, which can be followed in comparable regions.

2. GEOLOGICAL SETTINGS

The Komberek karst area, as well as the Malé Karpaty Mts., are integral parts of the Western Carpathian orogenic belt (Fig. 1). The geological structure of Malé Karpaty Mts. is divided into several tectonic units (Polák et al., 2011). The Tatricum tectonic unit is the most autochthonous unit and it is built by Paleozoic crystalline rocks and Mesozoic sedimentary cover rocks. The Fatricum and Hronicum tectonic units belong to the Western Carpathian nappe structures which were tectonically individualized during the Alpine orogeny in the Cretaceous period. In the studied area the Tatricum unit contains only its uppermost synorogenic flysch member, clayey shales, and turbiditic sandstones of Albian to Cenomanian age. An Upper Cretaceous thrust plane separates



underlying Tatric from Fatric unit in its hanging wall. The Komberek area (Fig. 2) is almost exclusively built up by the Fatric unit with Triassic and Jurassic to Cretaceous members. Middle Triassic dark-grey to black thick-bedded Gutenstein type limestone is the prevailing rock type in this area, and it also represents the lowermost part of Fatric unit. The tectonic contact between the Tatricum and the flysch sediments of the Fatricum units is linked to the rauhwackes. Rauhwackes (cornieules or cargneules) are breccias with a calcareous matrix that weather to form cavernous rocks. Very often they are associated with tectonic contacts. The origin of rauhwacke is still controversial but has been attributed to the weathering and alteration of dolomite-bearing evaporites, the tectonization of dolomites, or other processes (Krauter, 1971; Schaad, 1995). It is supposed that the rauhwackes are tectonically derived from the Gutenstein Limestones. The Gutenstein Limestones are commonly overlaid by Ramsau Dolomites. Variegated clayey shales, siliceous sandstones, and quartzites of

Fig. 1. a) Location of the study area in the Central European region. b) Study area of the karst plateau Komberek is situated in the northeastern part of the Malé Karpaty Mts.

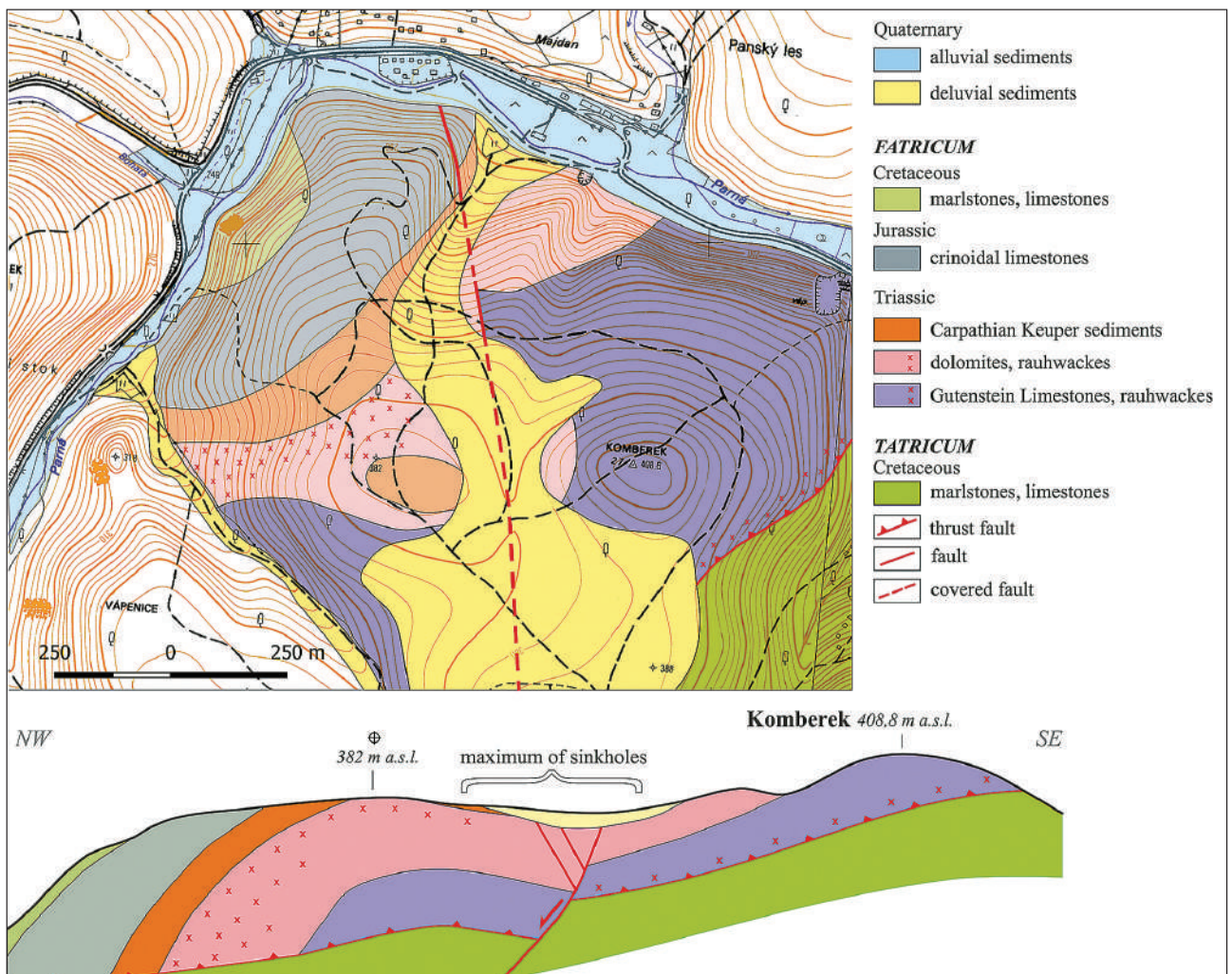


Fig. 2. Geological map with schematic cross-section of the study area. The cartographic background is elaborated according to <https://zbgis.skgeodesy.sk/mkzbgis/sk/zakladna-mapa>.

Upper Triassic age belonging to Carpathian Keuper Formation which overlies the Gutenstein and Ramsau carbonatic complex. In the north western part of the Komberek area Jurassic grey crinoidal cherty and nodular limestones occur. The Komberek area is disrupted by northwest–southeast-oriented normal faults active during the Neogene (Polák et al., 2012). The sinkholes are localized along lines situated on litological and tectonic discontinuities. The main lithological discontinuity is between the Carpathian Keuper Formation and the Ramsau Dolomites. The northwest-southeast tectonic line is the reason for the occurrence of the sinkholes array that follows it. The karst plateau is topped by a few meters thick cover of Quaternary deposits. These deposits are together with the karst landforms the main subject of this study. The Quaternary strata of the study area are until now poorly investigated, but the common presence of mudholes (explained below) and their lithology observed in speleological excavations indicate their fine-grained character.

3. GEOMORPHOLOGY AND KARST LANDFORMS IN THE STUDY AREA

The studied area belongs to the Kuchyňa-Orešany Karst (Stankoviansky, 1974). The northeastern part of Kuchyňa-Orešany Karst

is represented by the Komberek (Křč) Hill (409 m a.s.l.), which is a small (covering about 1 km²) but interesting karst plain (Fig. 2). Two caves, the Strapek Cave – backfilled (Fig. 3A, B) and the Závrtová Priepast Cave (Fig. 3C), were discovered. The karst platform represents a remnant of a pre-Pliocene planation surface (Stankoviansky 1974; Jakál et al., 1990; Minár et al., 2011). The surface of the karst plateau is situated 100 to 170 m above the recent Parná Stream and spans in altitudes of 370 to 406 m. a. s. l. Surface inclination reaches values of 0–8°. The plateau is adjacent to a mountain ridge which is situated on the southern part with altitudes up to 450–550 m. a. s. l.

Besides the caves, more than seventy terrain depressions were found in the area (Fig. 4), but some of them are not karst landforms, as they are man-made lime kilns (Putiška et al., 2014). The lime kilns were created to produce quick lime through the calcination of limestone. The kilns are up to 3 m in diameter and 1 m deep, which is very similar to some of the smaller natural sinkholes in the area. The original sinkholes as natural depression which could have been used as lime kilns as well. Several depressions are filled with mud and water, which makes it difficult to distinguish whether their origin is natural or not. The term mudhole will be used for these structures in the following text.

In the past, these sinkholes were described in the works of Droppa (1952), Novodomec (1967), Stankoviansky (1974),

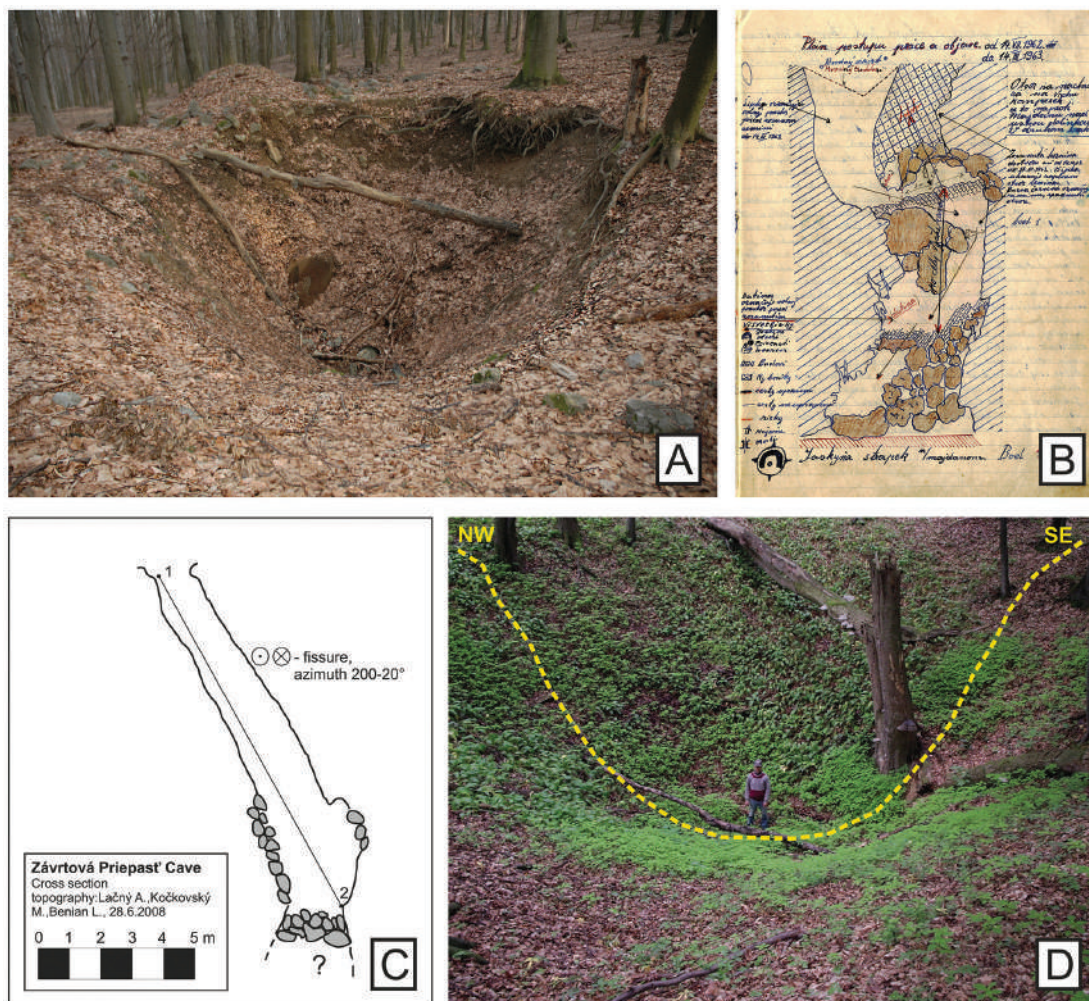


Fig 3.
 (A) Strapek Sinkhole.
 (B) Historical map of the backfilled Strapek Cave, mapped by P. Nemček.
 (C) Map of the Závrtová priepast Cave.
 (D) The largest sinkhole (KOM 30) in the Komberek karst area with localization of soil radon emanometry profile.

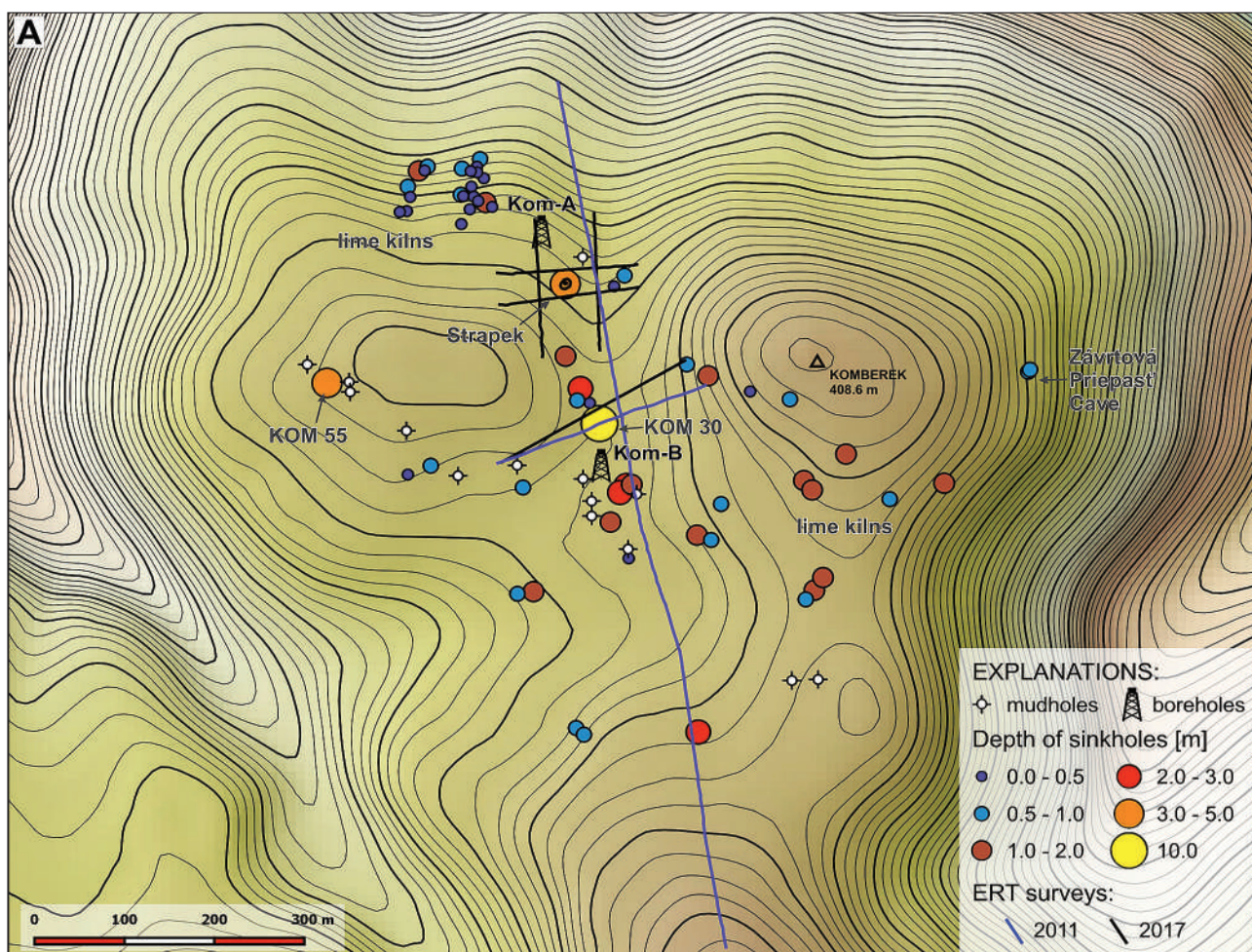


Fig. 4. Map of the Koberek area with distribution of sinkholes and mudholes, as well as with depicted ERT surveys and boreholes. Elevation contour step is 10 m (bold lines) and 2.5 m, respectively. (A) Spatial variation of a sinkhole depth.

Lačný (2007, 2008) and Šmída (2008). The sinkholes are 4–11 m wide and 0.5–3 m deep. One of the larger sinkholes (Strapek) was investigated by cavers led by P. Nemček (Nemček, 1967) and possibly earlier also by Vajsábel and Banič (Droppa, 1952). The largest of the sinkholes reaches a diameter of 26 m and a depth of 10 m (Fig. 3D).

Complexity of the geometry and spatial distribution of sinkholes, together with the various lithological composition of the basement rocks, outlines a question about factors affecting the genesis of the karst landforms. The presented study aims to investigate those issues.

4. METHODS

The standard methods and techniques of the geological mapping were used (in scale of 1: 10 000). The main portion of mapping activity was devoted to the internal structure of the Patricum tectonic unit, mutual contact between the Mesozoic sediments as well as kinematic character and age of surface visible (mappable) faults.

The main method of the geophysical research was the electrical resistivity tomography (ERT), which was implemented in two

phases. The first work was carried out in 2011 (partially published in Putiška et al., 2014), further detailed work was done during 2017. The ERT method allowed to obtain information on the distribution of the electrical resistivity in horizontal and vertical directions. The main principle of this measurement is the use of multiple grounded electrodes with the same distance between them and their subsequent connection to a multi-core cable (Griffiths and Barker, 1993). The measurements were made using the ARES II (GF Instrument) using Wenner-alpha electrode and dipole-dipole configuration. When using a large amount of measured data (resistivity cross section), it is possible to reconstruct the rock environment relatively well (Loke and Barker, 1995, 1996; LaBrecque et al., 1996). The realized geophysical measurements were positioned and height-oriented with Trimble GeoXR and Trimble M3v in the SJTSK coordinate system. The RES2DINV (Loke, 2010) application was used to interpret the measured values. The program creates a model where the calculated data are as close as possible to the measured data (Loke and Barker, 1996; Li and Oldenburg, 2000). When generating the model, the morphology of the terrain is also incorporated to the calculation.

A 235 m long profile with 5.0 m electrode step was measured at the KOM 30 sinkhole. Four additional profiles (ERT-P1 to ERT-P4) were measured in the vicinity of the Strapek sinkhole.

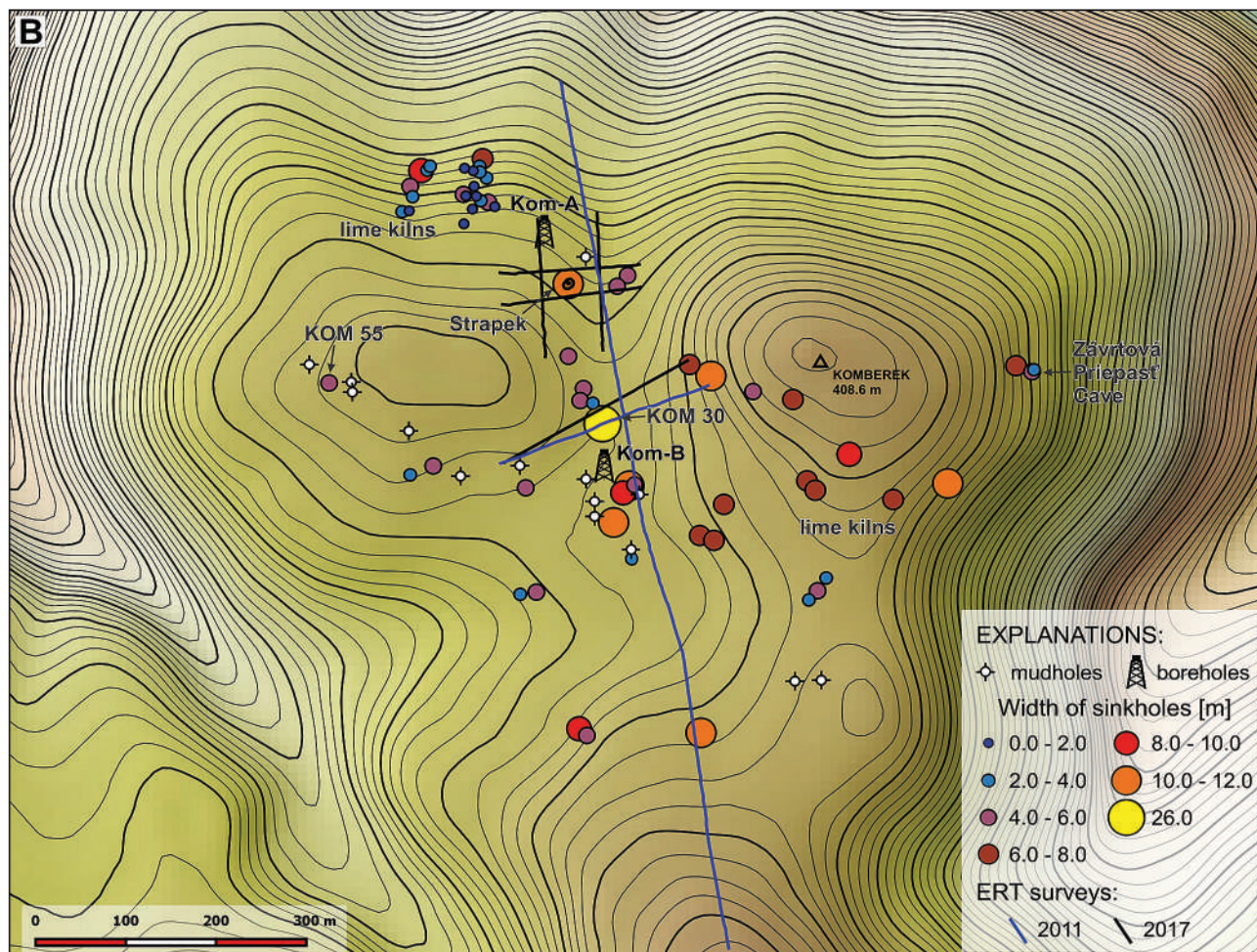


Fig. 4. Map of the Komberék area with distribution of sinkholes and mudholes, as well as with depicted ERT surveys and boreholes. Elevation contour step is 10 m (bold lines) and 2.5 m, respectively. (B) Spatial variation of a sinkhole width.

The length of the profiles was 156.0 m and the electrode step was 4.0 m.

As the additional method of the geophysical research the soil radon emanometry was applied. It is an atmogeochemical method that analyses a soil air sample for the presence of radioactive radon ($^{222}\text{Rn}_{86}$ isotope) emanation as a daughter product of ^{238}U disintegration in rock matrix. The amount of radon gas in soil air depends not only on uranium concentration in bedrocks, covers and soils but also on their permeability as radon gas has considerable ability to move upwards from extensive depths. This way the soil radon emanometry serves as a useful technique to trace places with higher air permeability due to weathering processes, tectonic disturbances or simply higher porosity, such as faults, disturbed zones, sinkholes, underground spaces, etc.

The measurements were made using the LUK 3R radon detector (SMM Prague, Czech Republic). The activity concentration of ^{222}Rn in soil air in kilo-Becquerels per cubic meter ($\text{kBq}\cdot\text{m}^{-3}$) was the measured variable. A 55 m long profile with 5–2 meters between single stations was measured cross the KOM 30 sinkhole in NW – SE direction. Soil air was sampled from the depth of approx. 0.8 m.

Quaternary sedimentary cover was studied using a shallow hand drill. The drilling equipment allowed to sample material in

20 cm steps. The obtained material was mixed in a 20 cm step and hence the primary depositional character was observable only in fragments of the cohesive sediment. The lithological log was created from visual observations of the drilled material. The clay versus silt content was estimated by hand. Furthermore, the fine fractions content was verified by six samples, which underwent sedimentation by the hydrometer method and sieving.

5. RESULT

5.1. Geological mapping

The results of geological mapping are depicted on the geological map at scale 1: 10 000 (Fig. 2). The area in question is build up by the Tatricum and Fatricum tectonic units, with significant presence of the Tatricum rock complexes.

5.2. Electric resistivity tomography surveys

The purpose of ERT profile measurements was to verify the geological structure in the vicinity of two mentioned sinkholes (KOM 30 and Strapek). The main task was to determine the

thickness of the cover structures and the presence of discontinuities (tectonic disturbances or lithological interfaces) on which the above-mentioned karst phenomena are developed.

The geological environment at the KOM 30 sinkhole is composed of two different environments with contrasting resistivities (Fig. 5A). To the east of the sinkhole the environment

is formed by rocks with a high resistivity value (above 500 $\Omega\cdot m$) correlated with compact carbonates. To the west of the KOM 30 sinkhole the environment changes and is formed by rocks with significantly lower resistivity values (5–300 $\Omega\cdot m$) which reach a thickness of 5 to 10 m in different parts of the section. The body may represent the Quaternary sedimentary

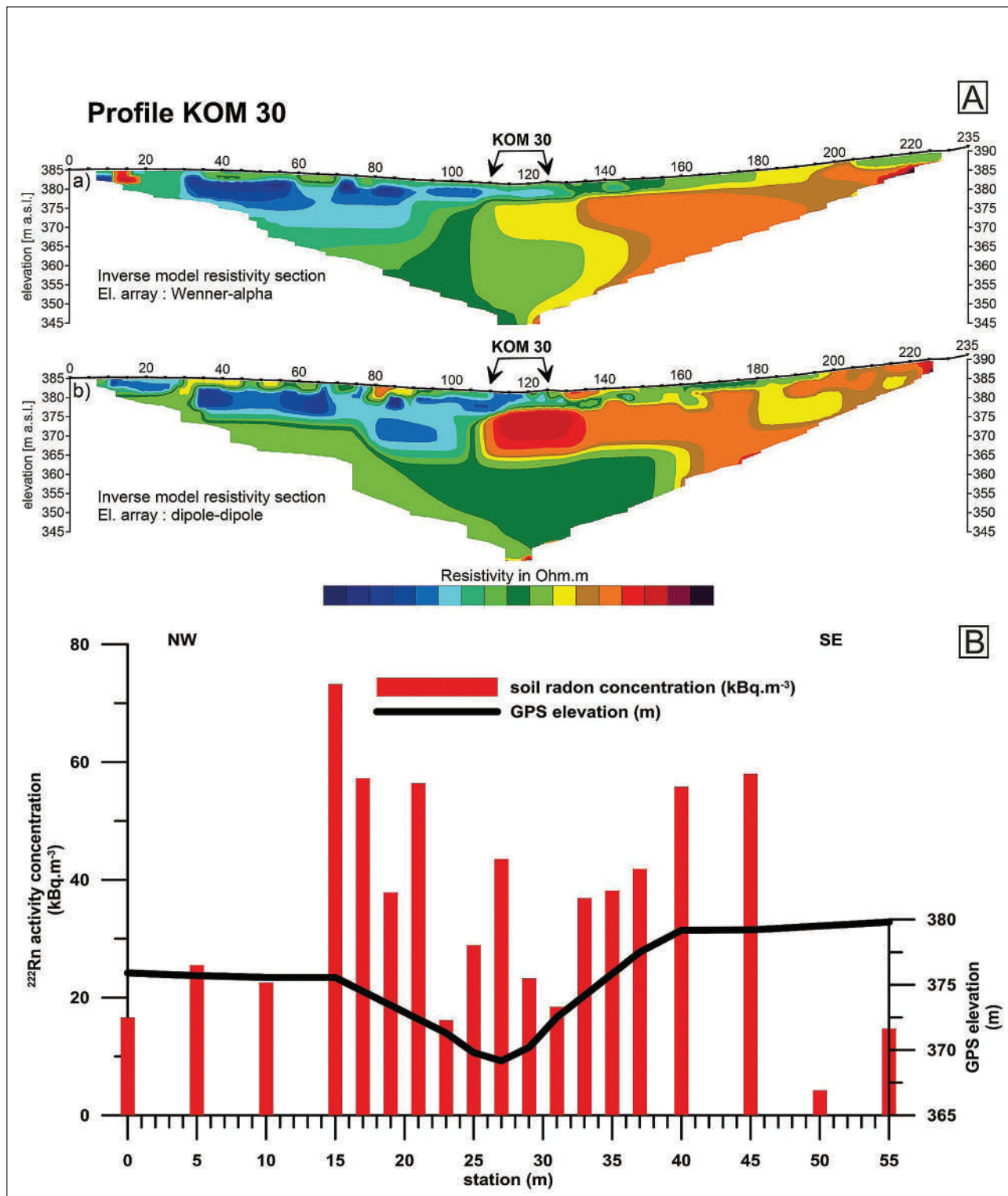


Fig. 5. (A) ERT results (profile KOM 30) –inverse resistivity cross sections. a) Wenner-alpha array, b) dipole-dipole array. (B) Soil radon emanometry results cross KOM 30 with topography of terrain.

fill of the depression. The sinkhole is located at the boundary of these environments. In the inverse line calculated from the dipole-dipole arrangements (Fig. 5A, below) a high resistivity anomaly is probably connected to a cavity under the sinkhole.

Similar situation is also found in the Strapek Sinkhole (Figs. 6 and 7), where the two profiles P1 and P2 located in an E-W

direction have revealed two different environments with distinct resistivity. To the east of the sinkhole an environment formed by compact rocks with a high resistivity values (above 500 Ω·m) occurs, to the east of the sinkhole is represented by an environment formed by rocks with a low resistivity values (5–300 Ω·m). Compact high resistivity environment was also confirmed

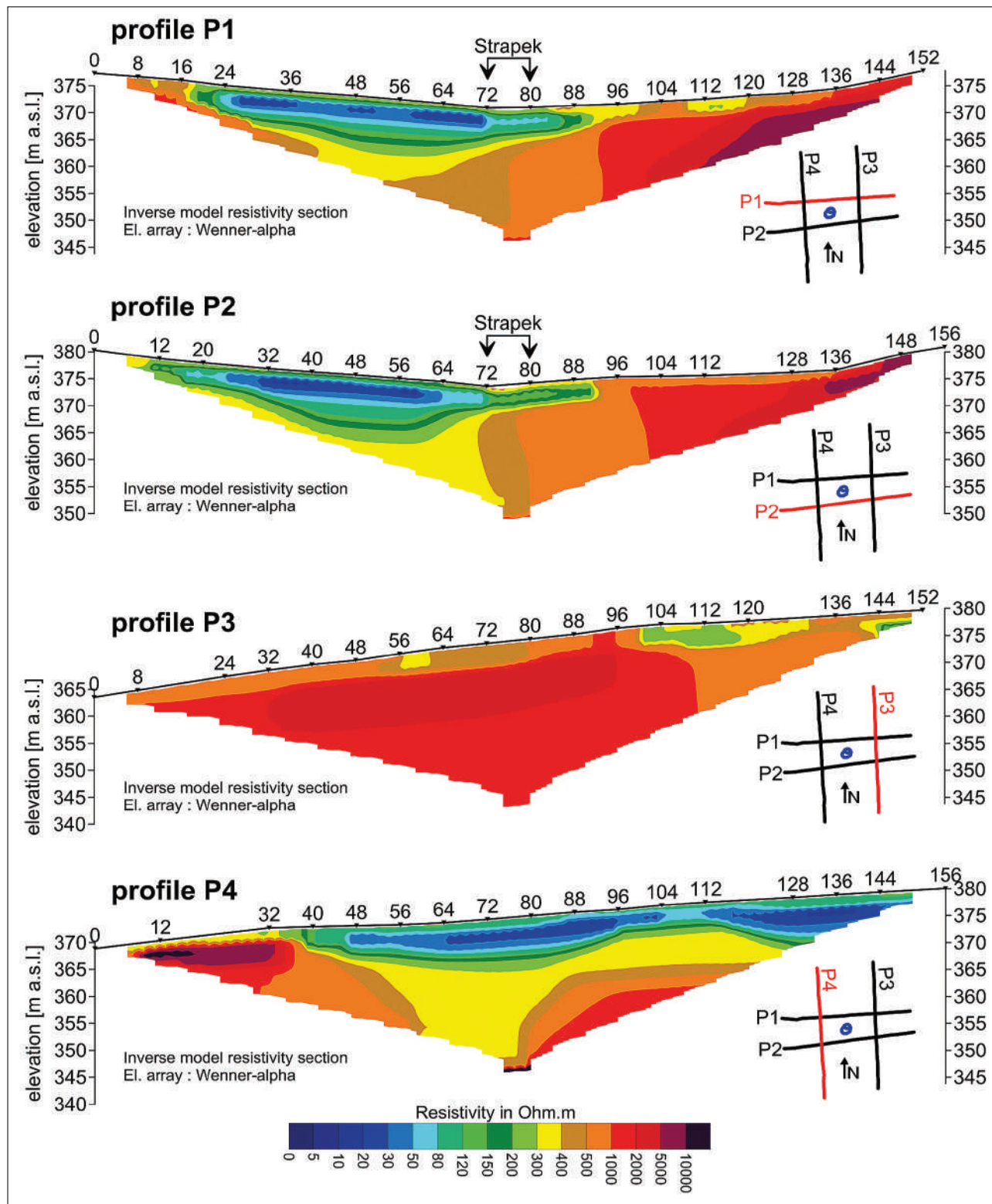


Fig. 6. ERT results (Strapek Sinkhole) – inverse resistivity cross sections for Wenner-alpha array.

by the P3 profile, which was located east of the sinkhole in an N–S direction. On the P4 profile, which was located to the west in an N–S direction, the presence of an environment with a low resistivity values were confirmed up from the 40th m meter to the end of the profile. The environment with low resistivity

has a thickness of 5–10 m. At the same time, there is an area with a high resistivity value (0–40 m), which is north from the sinkhole. It can be the associated with the same environment that is present east of the sinkhole.

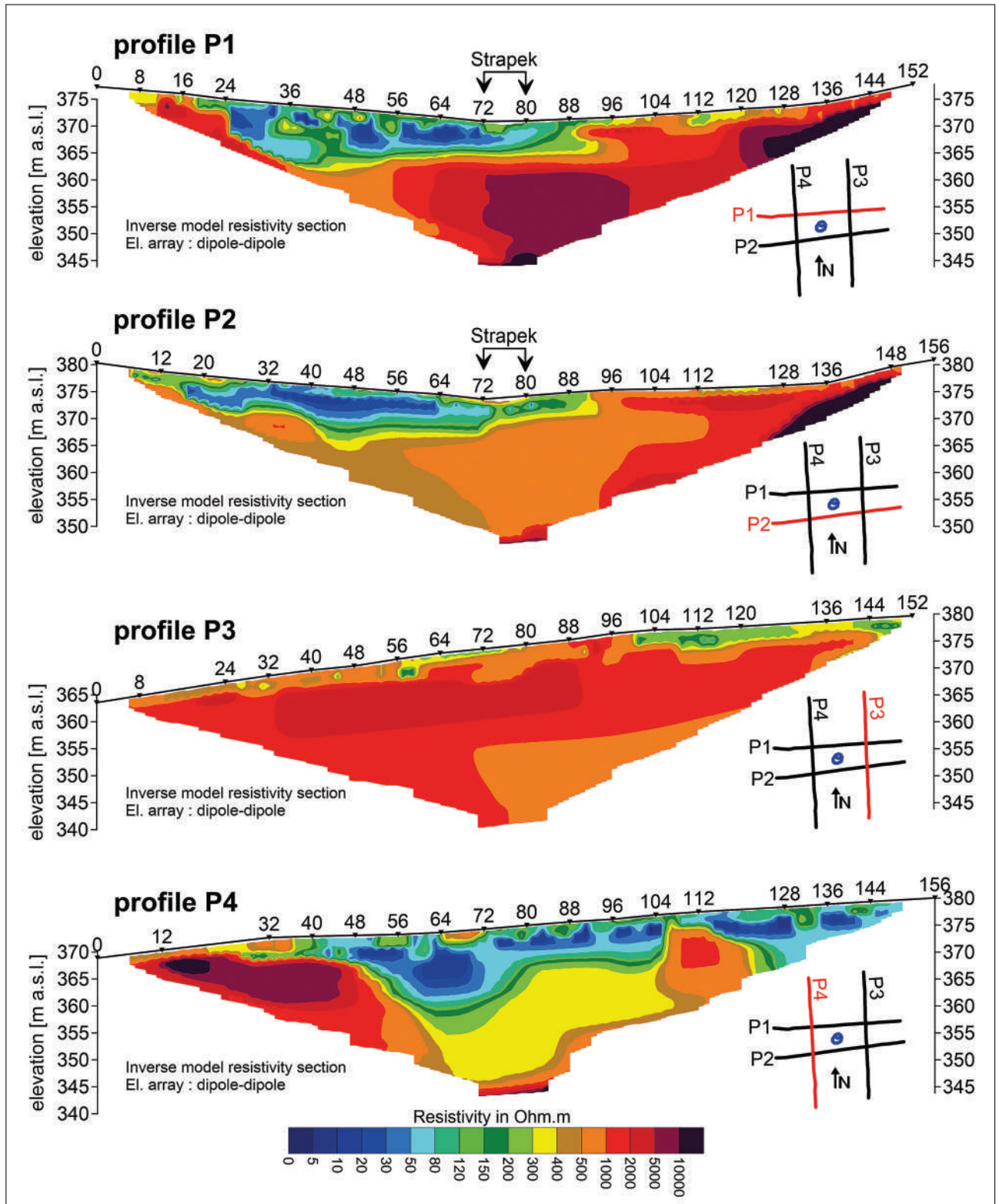


Fig. 7. ERT results (Strapek Sinkhole) – inverse resistivity cross sections for dipole-dipole array.

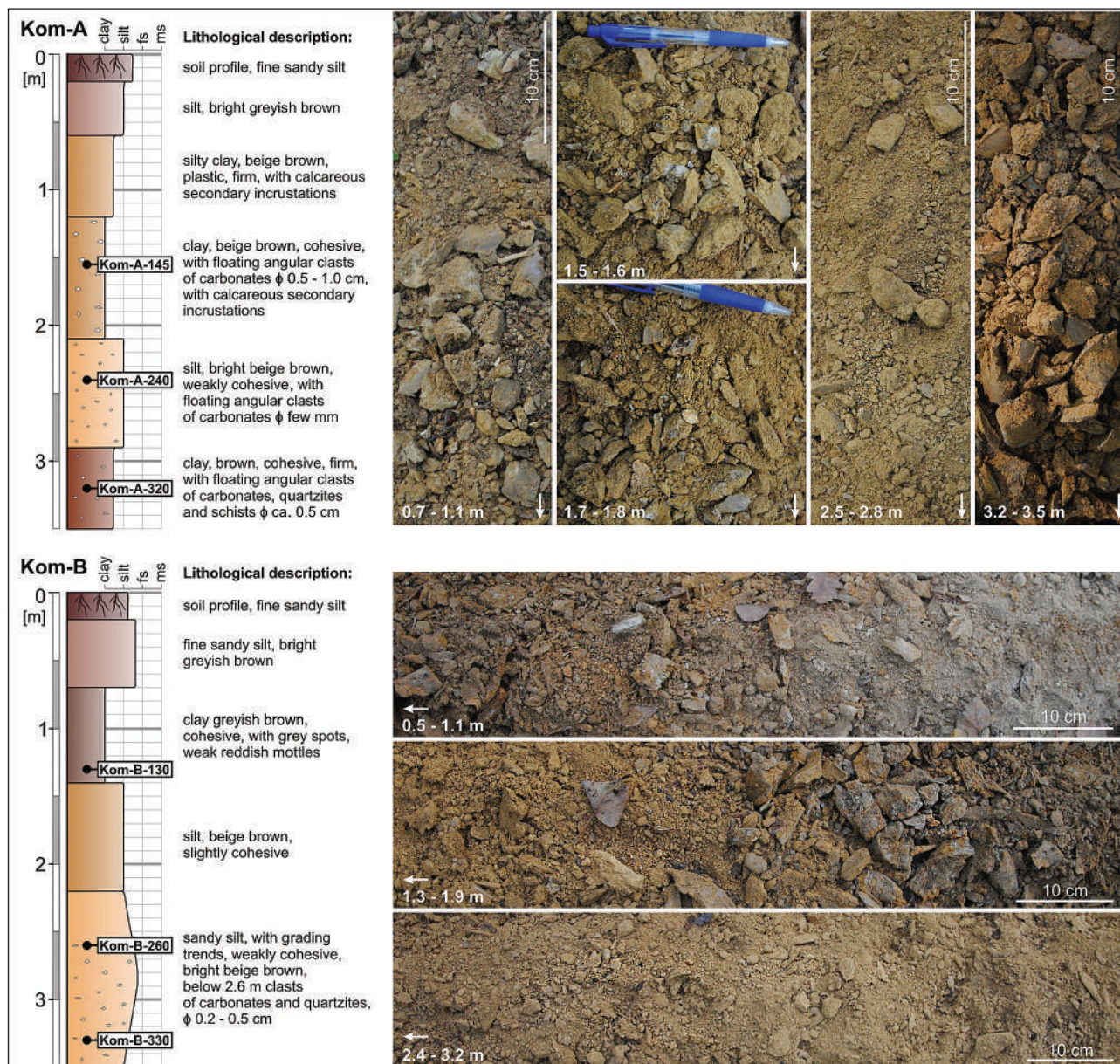


Fig. 8. Lithological logs obtained by hand drilling equipment, with indicated sampling points for granulometric analyses. Location of drillings is on Fig. 4. Precision of lithological changes is limited by 20 cm drilling steps. Photos of drilled material show variations in consistency (depending on content of fine fraction) and colour. Arrow is oriented downwards.

5.3. Soil radon emanometry measurements

The measurements of activity concentration of ^{222}Rn isotope in soil air were performed in detailed scale along a 55 m long profile cross the KOM 30 sinkhole in NW – SE direction (Fig. 3D) for the purpose to evaluate possible differences in cover and soil permeability between the sinkhole and its surroundings and to verify possible gas communication between sinkhole and its tectonic basement (Fig. 2).

The Figure 5B clearly documents strong difference in the soil radon concentrations (bar graph) between sinkhole and its surroundings. While the values outside the sinkhole (stations at 0, 5, 10, 50 and 55 m) reach from 4.2 to 25.5 $\text{kBq}\cdot\text{m}^{-3}$, with average of 16.7 $\text{kBq}\cdot\text{m}^{-3}$, those ones in the sinkhole (stations

at 15–40 m) range from 16.1 to 73.2 $\text{kBq}\cdot\text{m}^{-3}$, with average of 41.8 $\text{kBq}\cdot\text{m}^{-3}$. As such small survey area around KOM 30 sinkhole has homogeneous geochemical composition the soil radon concentrations' differences are attributed to differences in gas communication. Thus the sinkhole with higher permeability (thanks to karstic processes) undergoes better gas communication with underneath tectonics and is characterized by higher soil radon concentrations. The very opposite is valid for the sinkhole surroundings.

The radon bar graph also shows that the highest values of soil radon concentration are in the upper parts of sinkhole slopes (stations at 15–21 m and 33–45 m; with exception of 45 m that is not in the slope) which means the highest permeability and looseness. The lower parts of the sinkhole slopes (stations at 23,

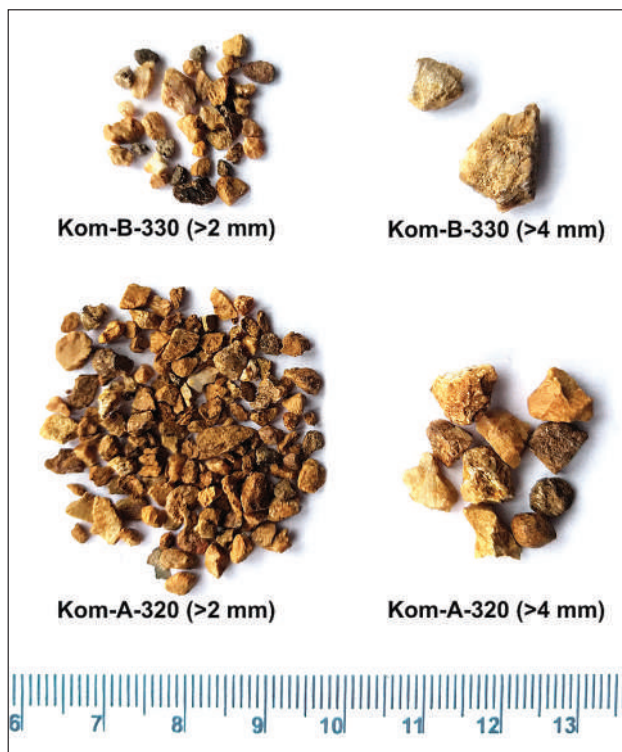


Fig. 9. Examples of angular clasts from drillings of mostly carbonates, with presence of quartzite and granitoides. Scale is in centimetres.

25, 29 and 31 m) are more tightened, with lower permeability, perhaps thanks to higher content of fine-grained particles, while the central bottom point (at 27 m) is again more loosened with higher radon concentration value. This behavior of soil radon concentrations crossing natural (tectonics) and man-made (coal mine) geological objects is partially documented in previous research works such as Mojzeš (2000), Pašteka et al. (2018) and Wysocka et al. (2018).

5.4. Sedimentary cover in drillings

Two locations for shallow drillings were selected, according to results from the ERT surveys, to investigate the character of the low resistivity rock environment. The material is generally composed of clays and silts with variable content of fine sandy admixture (Fig. 8). Angular floating clasts of carbonates, quartzites and schists are commonly present and reach dimensions of few mm up to 1 cm in diameter (Fig. 9). The probe Kom-A penetrated silts of grey colour, which gradually pass into cohesive beige brown clays in depth of 1.2–2.1 m. The content of floating clasts increases, as well as content of silt in interval 2.1–2.9 m, where sediment appears less cohesive. It is underlain by brown cohesive clays. The probe Kom-B penetrated cohesive grayish clays below sandy silt, followed abruptly by beige silt in the interval 1.2–2.2 m. The content of fine sand increases and floating clasts starts to appear in the lower portion of the drilling. Granulometric analysis revealed polymodal character of all six analyzed samples (Fig. 10). The most significant peak represents clay fraction, while the second most important is coarse silt. This peak comprises in samples Kom-B-260 and Kom-B-330 also very fine sand. Content of coarse sand is significant in samples Kom-A-240, Kom-A-320 and Kom-B-130. The granulometric analysis revealed, that the presence of floating clasts is minor regarding the weight percentage.

6. INTERPRETATIONS

Based on the above-mentioned results, the eastern part can be interpreted as a solid homogeneous carbonate massive (Fig. 11). A homogeneous rock mass can also be assumed in the western sections of the profiles. In the middle of the rock mass there is a depression filled with fine-grained sediments, characteristic with polymodal grain size distribution indicating polygenetic origin. High content of silt, together with the lithological nature

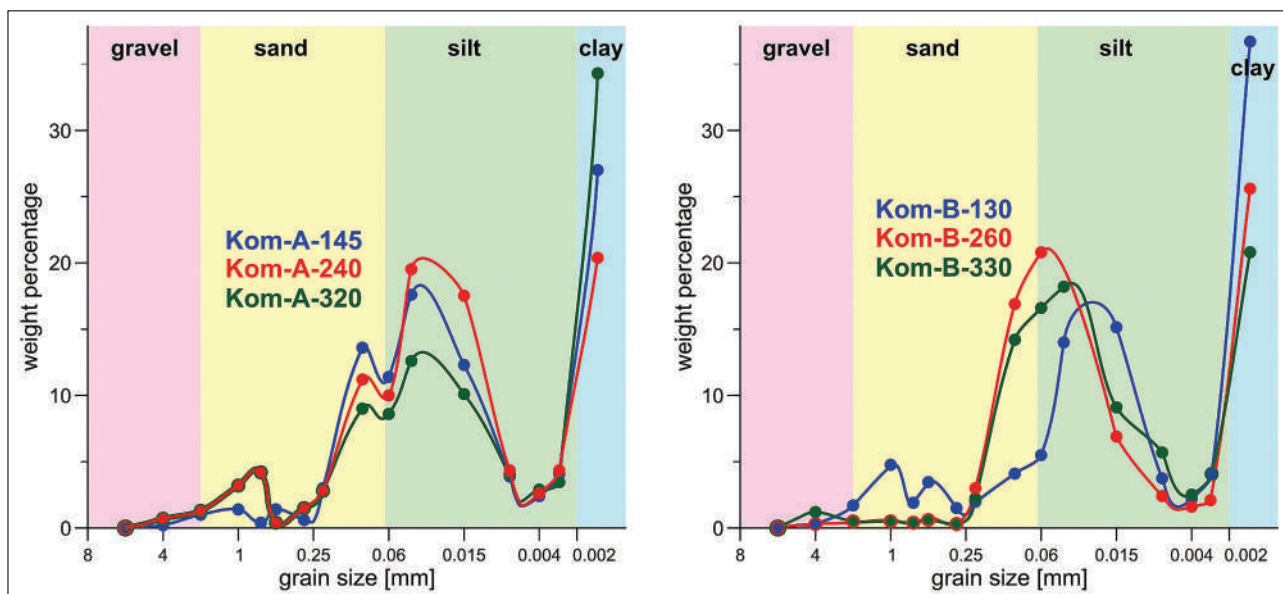


Fig. 10. Grain-size distribution of six samples taken from the drillings Kom-A and Kom-B (Fig. 8). Note the polymodal character of the deposit, which probably mirrors its polygenetic origin.

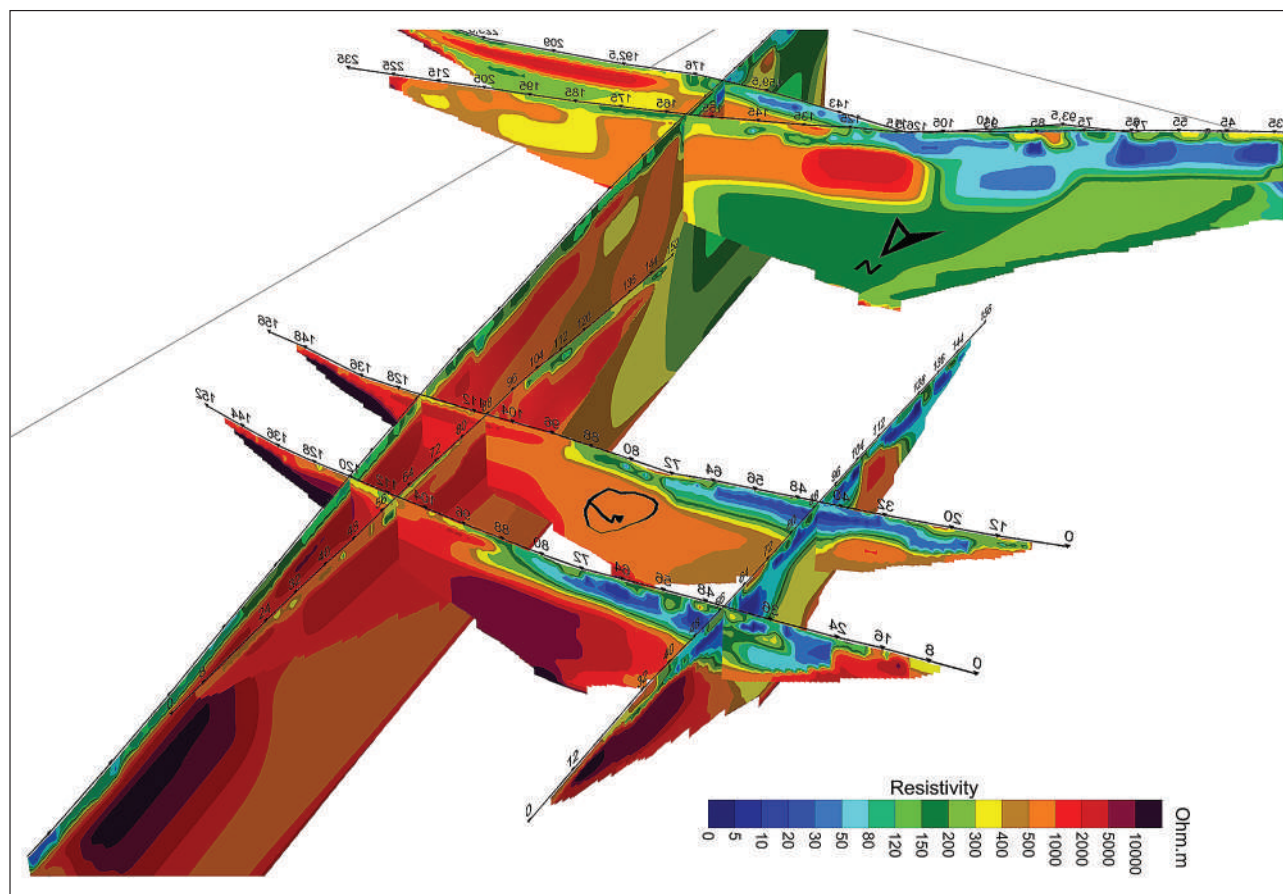


Fig. 11. The overall situation of all ERT profiles in the study area.

of observed strata, imply that these sediments are associated with redeposited loess. Dominance of clay fraction suggests intense weathering of the material, while angular character of the locally sourced floating clasts is an evidence of very short transport, probably by a surface runoff. The sediments may be the result of a low-dynamic, long-term process of redeposition on a low angle slope platform which is affected by partial topographic isolation from further high angle slopes situated to the south. The input of clastic material decreased with time, as could be seen from vertical succession logged in the probes.

This depression possibly arose as a consequence of a significant fault structure of a NW–SE direction dipping to southwest (Fig. 2). The results from field geological mapping imply that the structure has normal kinematics. The significant depths and diameters of sinkholes are concentrated in a NW–SE line, which corresponds to the carbonate contact zone disrupted by fault. Supporting evidence is provided by soil radon measurements with significantly higher values in the sinkhole in comparison with markedly lower values beyond it. The abundance of sinkhole soil radon gas has to be rooted in underneath fault. At the same time, the line forms the lowest morphological point, where the highest drainage and infiltration of water into the underground occurs. This results in vertical distribution of soil particle size inside the sinkhole where the coarse-grained material covers the upper parts of sinkhole slopes while the fine-grained one lies in the lower parts of slopes and bottom of the sinkhole (Fig. 5B). Further to the west, fine-grained Quaternary sediments form

a natural isolator against precipitation infiltration, which can significantly affect the intensity of karst processes under these sediments.

However, the slopes on the karst plateau reach an average diameter of 4–11 m with depths of 0.5–3 m (Fig. 12). They concentrate especially south-east of the sinkhole line, excluding limestone pits south of Komberek Hill. They are formed by shallow depressions, often filled with mud, in which water is partly held (Fig. 13). In these portions, the largest accumulations of sediments occur (5 to 10 m thick). We infer that the sinkholes also follow a discontinuity in the basement. As a result of the coverage by fine-grained sediments, the karst processes are limited, and the slopes tend to dip more moderately than their equivalents found at the edge of depression which are in contact with the carbonates (Fig. 14).

It can be assumed that, before the depression opened (before fault movement) the rock mass was exposed on both sides of the fracture. Thus, the karst processes could have had a similar intensity. After the deposition of the fine-grained sediments, the karst processes were significantly limited in this zone, but the depressions are still situated above the sinkholes located in the basement. The creation of an impermeable sediment body had the opposite effect on the formation of sinkholes directly at the fault, where the increased infiltration made karst processes more intense.

It is also important to mention occurrence of a sinkhole (KOM 55), which is located in the western part of the plateau and is

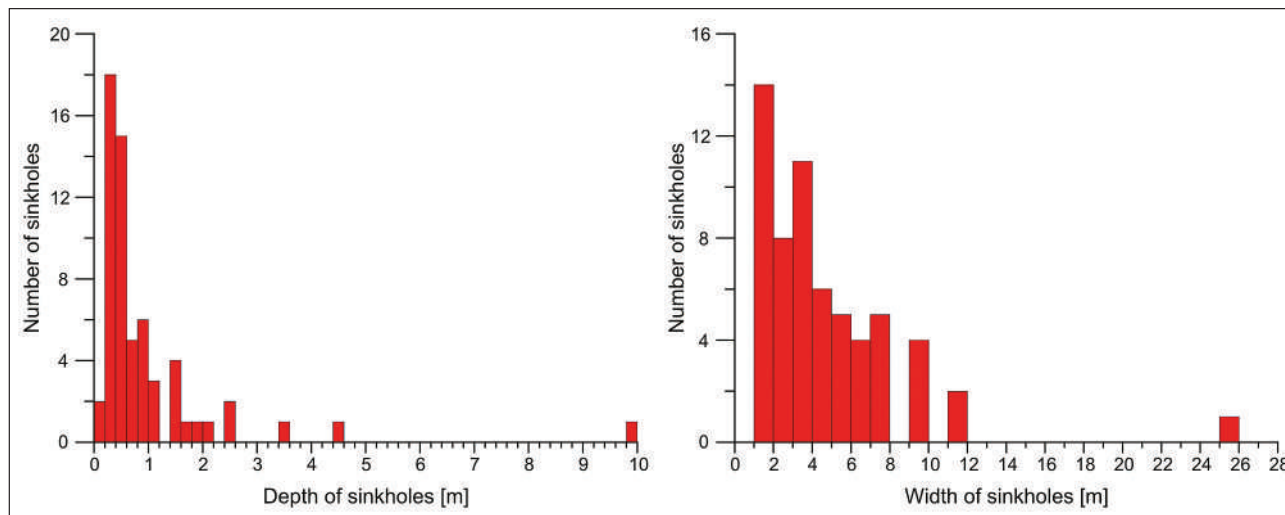


Fig. 12. Histograms of depth and width of sinkholes in the study area.

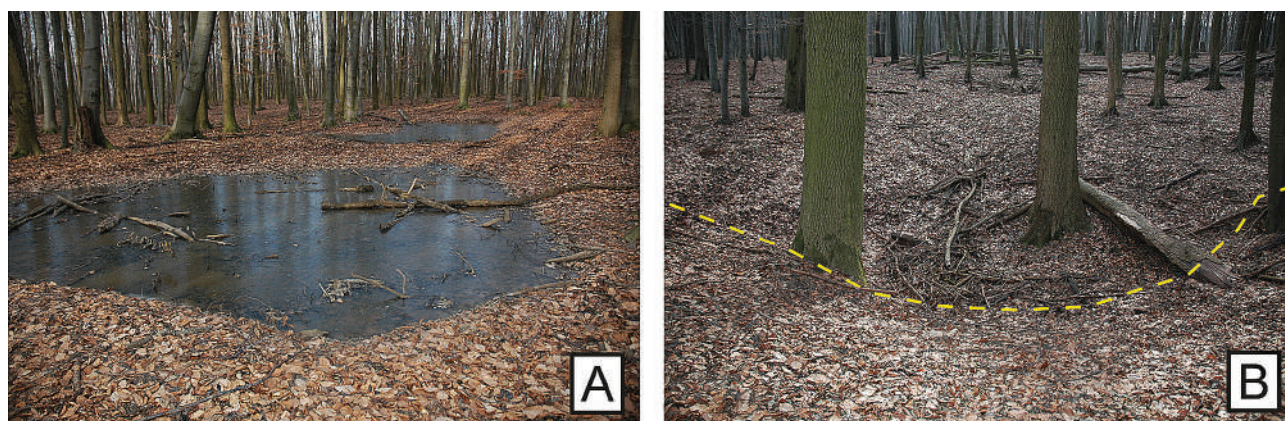


Fig. 13. (A) Mudhole with water and (B) shallow sinkhole localized in the southeastern part of the Komberek karst area (yellow line represent morphology).

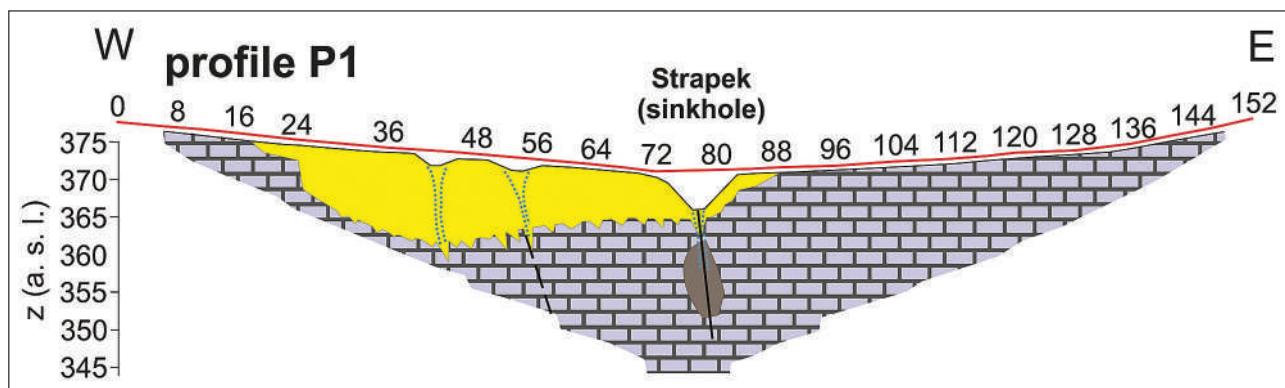


Fig. 14. Interpretation origin of sinkholes in the profile P1 near Strapek with backfilled Strapek Cave.

formed on the lithological boundary of the Carpathian Keuper and carbonates. At the site the Carpathian Keuper is formed mainly by reddish shales and quartzites. On the surface the red shales denudate rapidly and leave behind a characteristic red colored. This makes direct field determination possible where the red color reveals the presence of a nearby outcrop, where sinkholes may have originated on a lithological boundary of karstic and nonkarstic rocks.

7. CONCLUSIONS

A case study of the Komberek karst plateau was performed by using methods of field geological research and geophysical survey methods (the ERT method and the soil radon emanometry). Based on the obtained results it was possible to interpret the origin and morphology of the sinkholes which depends on the nature of the basement rocks, the sedimentary cover and the

tectonic influence. In terms of the Jakál's classification (Jakál, 1975), funnel-shaped and pot-like sinkholes are concentrated into a sinkhole line located at the edge of the depression filled with fine-grained impermeable sediments; on the contrary, the bowl-like sinkholes, are often connected to swampy areas where the basement reaches highest thickness. The sinkholes were created by the slow corrosive effect of water on tectonic or lithological discontinuities. A linear NW–SE-trending structure seems to be controlling the karst forms in this area. The above-mentioned discontinuities also developed sinkholes in a lines in the Biela skala and Dlhý vrch area of the Kuchyňa-Orešany Karst (Veselský et al., 2014a, b). Furthermore, this study highlights the possible presence of cave spaces under the largest of the sinkholes found on the karst plateau. The possible cave spaces are located in the KOM 30 and Strapek sinkholes. Nevertheless, an interesting problem remains, where is the surface infiltrated water further drained? It is likely to have a deeper circulation, as there is no significant karst spring in the vicinity of the platform which would be connected to this area.

ACKNOWLEDGMENT

This work was supported financially by the Slovak Research and Development Agency under the contracts APVV-0099-11, APVV-14-0118, APVV-15-0575, APVV-16-0121, APVV-16-0146 and SK-FR-2015-0017 as well as by the Scientific Grant Agency of the Ministry of Education, Science, Research and Sport of the Slovak Republic and the Slovak Academy of Sciences (VEGA) within the project 1/0602/16, VEGA 1/0462/16, 1/0559/17 and 1/0115/18.

REFERENCES

- Bondesan A., Meneghel M. & Sauro U., 1992: Morphometric analysis of dolines, *International Journal of Speleology*, 21, 1–55.
- Droppa A., 1952: Kras na juhovýchodnej strane Malých Karpát. In: Virsik M. et al. (Eds.): Kras a jaskyne Malých Karpát. [The karst on the southwestern part of the Malé Karpaty Mts. In: Virsik M. et al. (Eds.): The karst and caves in Malé Karpaty Mts.] Sprievodca Slovakotouru. Tatran, Bratislava, 63–138. [in Slovak]
- Griffiths D.H., Barker & R.D., 1993: Two-dimensional resistivity imaging and modelling in areas of complex geology. *Journal of Applied Geophysics*, 29, 211–226.
- Jakál J., 1975: Kras Silickej planiny. [Karst land of Silická planina] Osveta, Martin, 149 p. [in Slovak]
- Jakál J., Lacika J., Stankoviansky M. & Urbánek J., 1990: Morfoštruktúry Malých Karpát. [Morphostructures of the Malé Karpaty Mts.] Manuscript, Geografický ústav SAV, Bratislava, 163 p. [in Slovak]
- Krauter E., 1971: Zur Genese rauhwackiger Breccien der alpinen Trias an Beispielen aus der Schweiz und Österreich: *Geologisch-Palaontologische Mitteilungen*, Innsbruck, 1(7), 11.
- LaBrecque D., Miletto M., Daily W., Ramirez A. & Owen E., 1996: The effects of Occam's Inversion of resistivity tomography data. *Geophysics*, 61, 538–548.
- Lačný A., 2007: Kuchynsko-orešanský kras v rajóne OS Dolné Orešany. [Kuchyňa-Orešany Karst in the region of the Dolné Orešany] *Spravodaj Slovenskej speleologickej spoločnosti*, 38, 53–57. [in Slovak]
- Lačný A., 2008: Zhrnutie doterajšieho speleologického prieskumu na Komberku. [A summary of the current speleological survey at Komberk hill] *Spravodaj Slovenskej speleologickej spoločnosti*, 39, 35–37. [in Slovak]
- Li Y.G. & Oldenburg D.W., 2000: 3-D inversion of induced polarization data. *Geophysics*, 65, 1931–1945.
- Loke M.H. & Barker, R.D., 1995: Least-squares deconvolution of apparent resistivity pseudosections. *Geophysics*, 60, 1682–1690.
- Loke M.H. & Barker R.D., 1996: Rapid least-squares inversion of apparent resistivity pseudosections by a quasi-Newton method. *Geophysical Prospecting*, 44, 131–152.
- Loke M.H., 2010: Tutorial: 2-D and 3-D electrical imaging surveys. www.geoelectrical.com/downloads.php, 08.02.2011.
- Minár J., Bielik M., Kováč M., Plašienka D., Barka I., Stankoviansky M. & Zeyen H., 2011: New morphostructural subdivision of the Western Carpathians: An approach integrating geodynamics into targeted morphometric analysis. *Tectonophysics*, 502(1–2): 158–174.
- Mojžeš A., 2000: Možnosti hodnotenia fyzikálneho stavu horninového masívu z hľadiska jeho rádioaktivity. [The possibilities of evaluation of physical state of rock massif from the point of its radioactivity.] In: Lučivjanský L. (Ed): Proceedings of the 2-nd Conference „Radioactivity in Environment, Spišská Nová Ves, 112–114. [in Slovak]
- Nemček P., 1967: Pracovný denník skupiny Strapek. [Workbook of group Strapek] Manuskript, archív SMOPaJ, Liptovský Mikuláš, non-paged document. [in Slovak]
- Novodomec R., 1967: Geomorfologické pomery povodia Parnej v Malých Karpatoch. [Geomorphological conditions of Parná river catchment in the Malé Karpaty Mts.] *Geografický časopis*, 19, 212–223. [in Slovak with English abstract]
- Pašteka R., Záhorec P., Papčo J., Kušnirak D., Putiška R., Mojžeš A., Zvara I., Leško M., Bielik M. and Plakinger M., 2018: Experiences from Microgravity Method Application in Abandoned Coal Mine Sites – Two Examples from Austria and Slovakia. In: Proceedings of the Near Surface Geoscience Conference and Exhibition 2018, 24-th Meeting of the European Association of Environmental and Engineering Geophysics, Porto, Portugal, We 24P2 01, 1–5.
- Polák M., Plašienka D., Kohút M., Putiš M., Bezák V., Filo I., Olšovský M., Havrila M., Buček S., Maglay J., Elečko M., Fordinál K., Nagy A., Hraško L., Németh Z., Ivanička J. & Broska I., 2011: Geological map of the Malé Karpaty Mts. (scale 1:50 000). State Geological Institute of Dionýz Štúr, Bratislava.
- Polák M., Plašienka D., Kohút M., Putiš M., Bezák V., Maglay J., Olšovský M., Filo I., Havrila M., Buček S., Elečko M., Fordinál K., Nagy A., Hraško L., Németh Z., Malík P., Liščák P., Madarás J., Slavkay M., Kubeš P., Kucharič L., Boorová D., Zlinská A., Siráňová Z. & Žecová K., 2012: Explanatory notes to the geological map of the Malé Karpaty Mts. in scale 1 : 50 000.-State Geological Survey of Dionýz Štúr, Bratislava, 287 p. [in Slovak with English summary]
- Putiška R., Kušnirak D., Dostál I., Lačný A., Mojžeš A., Hók J., Pašteka R., Krajňák M. & Bošanský M., 2014: Integrated geophysical and geological investigations of karst structures in Komberk, Slovakia. *Journal of Cave and Karst Studies*, 76(1), 155–163.
- Schaad W., 1995: Die Entstehung von Rauhwacken durch die Verkarstung von Gips, *Eclogae Geologicae Helveticae*, 88, 59–90.
- Stankoviansky, M., 1974: Príspevok k poznaniu krasu Bielych hôr v Malých Karpatoch. [Contribution to the knowledge of the Biela hora karst in the Malé Karpaty Mts.] *Geografický časopis*, 26, 241–257. [in Slovak with English abstract]
- Šmída B., 2008: Krasové jamy (závrty) Západných Karpát: štúdium ich morfológie a genézy. [Sinkholes of the Western Carpathians: the study of the morphology and genesis] Minimum thesis, Faculty of Natural Sciences, Comenius University in Bratislava, 113 p. [in Slovak]

- Veselský M., Ágh L., Lačný A. & Stankoviánsky M., 2014a: Závrtý na krasovej plošine Biela skala a ich morfometrická analýza, Kuchynsko-orešánský kras, Malé Karpaty. [Sinkholes on the karst land of Biela skala and morphometric analyses, Kuchyňa-Orešany Karst, Malé Karpaty Mts.] *Slovenský kras*, 52, 127–139. [in Slovak with English summary]
- Veselský M., Lačný A. & Hók J., 2014b: Závrtý na Dlhom vrchu: modelová štúdia ich vzniku na lineárnych diskontinuitách (Malé Karpaty). [Dolines on Dlhý vrch hill: case study of doline evolution on linear discontinuity (Malé Karpaty Mts.)] *Acta Geologica Slovaca*, 6, 159–168. [in Slovak with English summary]
- Williams P., 2004: Dolines. In: Gunn J. (Ed.): *Encyclopedia of Caves and Karst Science*. Taylor and Francis Group, London, 304–310.
- Wysocka M., Skubacz K., Chmielewska I., Bonczyk M., Urban P. and Grycman J., 2018: Changes in radon emission in the area around the coal mine during closing process. In: Barnet I., Neznal M. and Pacherová P. (Eds.): *Proceedings of the 14-th International Workshop on the Geological Aspects of Radon Risk Mapping*, Prague, pp. 158–164.